https://doi.org/10.1038/s41467-022-32131-4

The defect challenge of wide-bandgap semiconductors for photovoltaics and beyond

Alex M. Ganose, David O. Scanlon, Aron Walsh and Robert L. Z. Hoye

The optoelectronic performance of wide-bandgap semiconductors often cannot compete with that of their defect-tolerant small-bandgap counterpart. Here, the authors outline three main challenges to overcome for mitigating the impact of defects in wide-bandgap semiconductors.

Visible-light harvesting materials with bandgaps in the range of 1.6–2.5 eV are gaining increasing significance across a range of emerging technologies, such as indoor and tandem photovoltaics (PVs), but feature inferior optoelectronic performance compared to their small-bandgap (<1.6 eV) counterparts. Charge-carriers tend to have shorter diffusion lengths, along with higher trapping and recombination rates. We outline the critical challenges for achieving defect-tolerant wide-bandgap crystals, and suggest promising routes forward.

Efficient, low-cost devices through defect tolerance

Defects are ubiquitous in crystalline semiconductors. Managing their influence on electronic properties is critical for high performance across a range of technologies, including PVs, photoelectrochemical cells and radiation detectors. Of particular importance are point defects—including vacancies, anti-sites or interstitials—which lead to the introduction of electronic states that fall within the bandgap (E_g), resulting in irreversible losses in charge-carriers through trapping and non-radiative recombination. Historically, the effects of defects were mitigated by minimising their concentration through careful (and often expensive) fabrication methods, such as the case for Si[1]. More recently, new classes of semiconductors have been discovered that can maintain high light conversion efficiency despite high concentrations of point defects. Such defect tolerance can arise in several ways. Defects can pair together to form electronically benign complexes (e.g., in $CuInSe_2$)[2,3]. Defects can also be less harmful if: (i) the dominant traps within the bandgap are energetically close to the valence or conduction band edges (i.e., shallow), or (ii) have low capture cross-sections (see ref. 4 for details). These effects have been found in metal-halide perovskites, and are an important factor behind their rapid achievement of PV efficiencies comparable to those of Si[1,4], despite being processed at significantly lower temperatures that enable lower levelised cost of energy and CO_2eq footprint[5].

Wide-bandgap challenge

Semiconductors that have both been demonstrated to be defect tolerant and also realised in efficient PV (i.e., $CuInSe_2$ and iodide-based perovskites) have only been achieved for materials with <1.6 eV bandgap[1–3]. Wider-bandgap semiconductors, with E_g in the range of 1.6–2.5 eV, have had less success, but are now becoming increasingly important for a range of clean energy and healthcare applications. These include indoor PV (optimal E_g of 1.9 eV) to sustainably power the Internet of Things[6], photoelectrochemical cells (~2 eV) for single-junction solar-to-hydrogen water splitting[7], X-ray detectors (1.4–2.5 eV) for medical imaging and security[4], and top-cells (>1.7 eV) for tandem PV with silicon[8]. There are a number of obstacles to overcome. Below, we discuss the critical challenges to achieving defect tolerance in wide-gap semiconductors, and inspiration on how these challenges could be overcome.

Harder dopability. Many materials can be doped by either electrons (n-type) or holes (p-type) but not both. Such doping asymmetry is a feature of wide-bandgap systems. One example is the field of transparent oxide electronics where n-type doping is possible (e.g., in ZnO, SnO_2, In_2O_3), yet effective p-type doping is much more challenging. This type of behaviour is often rationalised by using the doping limit rules[9] (and sometimes explained by the concept of Fermi level pinning), which state that the lower the ionisation potential (valence band energy), the easier it is to make a material p-type, and the higher the electron affinity (conduction band energy), the easier it is to make it n-type. The limit itself is imposed by the spontaneous formation of charge compensating point defects. As such, wide-gap semiconductors with low electron affinity and/or high ionisation potential generally have lower dopability to one or both carriers. This can be seen in Fig. 1a, in which there is an overall decrease in the predicted dopability ($\delta\varepsilon_F$) as the bandgap increases (especially for the case of p-type dopability shown)[10]. Whilst the correlation between band-edge position and dopability is established, the link between dopability and defect tolerance is still unresolved.

Increased ionicity. Ionic materials typically have larger bandgaps than their covalent counterparts, which can be seen, for example, in comparing NaCl (8.5 eV) to silicon (1.12 eV), or LiF (14 eV) to diamond (5.5 eV). As charge transfer increases, a stronger Coulomb potential separates the valence and conduction bands. For example, the bandgap of $CH_3NH_3PbI_3$ can be continuously increased from 1.59 to 3.04 eV by changing the halide species to the more electronegative Br or Cl, or using mixtures thereof (Fig. 1b)[11]. The established defect tolerance of $CH_3NH_3PbI_3$ is not preserved across the entire halide composition range. The halide vacancy (0/+) donor level becomes deeper through the series (Fig. 1b), due to the lower electron affinity, as well as the smaller lattice constant of $CH_3NH_3PbCl_3$ leading to greater overlap between Pb dangling bonds when halide vacancies form[12]. The electrostatic potential at the vacancy site becomes sufficiently large to localise an unpaired electron to form a deep state with large structural relaxation energy. For the case of $ZnO_{1-x}S_x$, a nitrogen acceptor is deep above the valence band for small values of x, but becomes shallower for S-rich materials[13]. Increased ionicity can lead to stronger carrier trapping and activate

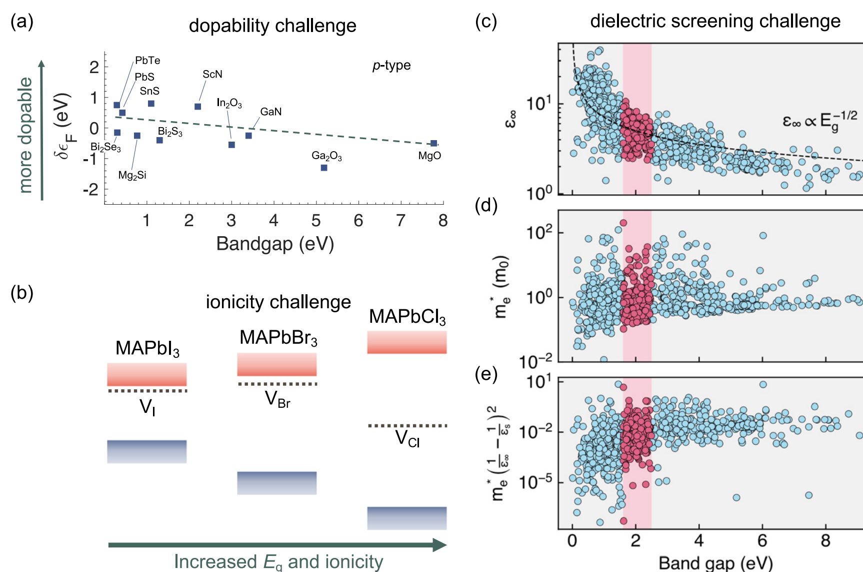

Fig. 1 | The defect challenge for wide-gap semiconductors. a Dopability challenge. Plot of the ability to dope materials ($\delta\varepsilon_F$) as a function of their bandgap (E_g). $\delta\varepsilon_F$ is defined as the difference between the band-edge (valence band maximum for p-type doping) and doping pinning energy. $\delta\varepsilon_F$ from defect calculations in ref. 10, while the bandgaps shown are experimentally measured values. Trend line added to guide the eye. **b** Ionicity challenge. Energy of the (0/+) transition level of the halide vacancy for $CH_3NH_3PbX_3$ perovskites. Dielectric screening challenge. **c** Plot of electronic dielectric constant (ε_∞), **d** electron effective mass (m_e), and **e** Fröhlich polaron binding energy factor (in which ε_S is the static dielectric constant) against bandgap for binary compounds in the Materials Project database[20]. The shaded red regions highlight the bandgap range 1.6–2.5 eV of interest. The data for panels **c**–**e** were calculated using density functional theory within the generalised gradient approximation. Whilst bandgaps are underestimated, the underlying physical trends are expected to be valid. Effective mass and dielectric tensors were isotropically averaged.

previously benign defects for non-radiative electron-hole recombination pathways.

Weaker dielectric screening. As the bandgap of a material increases, the polarisability also tends to decrease. Indeed, the high-frequency dielectric constant is inversely proportional to the square-root of the bandgap (Fig. 1c). There is also a correlation with effective mass as the interaction between the valence and conduction band edges is weakened (Fig. 1d). Defect tolerance requires low charge capture cross-sections, which are strongly influenced by both the dielectric constant and effective mass of the host material. A large dielectric constant screens electrostatic interactions between charged defects and charge-carriers, and maintains a low Sommerfeld factor (see ref. 4 for further details). A low effective mass m_0^* facilitates high mobilities and enhances the delocalisation of the defect wavefunctions with the band edges. These factors also control the degree of polaron formation, which in the simplified Fröhlich model gives the relation.

$$E_p \propto m_0^* \left(\frac{1}{\varepsilon_\infty} - \frac{1}{\varepsilon_s}\right)^2 \quad (1)$$

where E_p is the polaron binding energy, and ε_s and ε_∞ are the static (low-frequency) and high-frequency dielectric constants, respectively. This relationship presents a challenge, as based on these considerations, wide-gap materials should have less mobile charge-carriers (as seen from the positive correlation between E_p and E_g in Fig. 1e) with higher recombination rates (due to the smaller dielectric constants and larger effective masses). Even in the case of III–V semiconductors, the exceptional 9000 $cm^2 V^{-1} s^{-1}$ electron mobility for GaAs (E_g = 1.5 eV, m_e = 0.07, ε_∞ = 10.9) is reduced to 900 $cm^2 V^{-1} s^{-1}$ for GaN (E_g = 3.5 eV, m_e = 0.22, ε_∞ = 4.9)[14].

Future opportunities

A promising avenue to enhance dielectric screening is to identify host materials with large ionic (vibrational) contributions to the static dielectric constant. This component is sensitive to the underlying structure and vibrations, which can be tuned through crystal engineering. The net ionic screening (defined as $\varepsilon_s - \varepsilon_\infty$) is decoupled from the bandgap (Supplementary Fig. 1). Instead, large ionic contributions are found in materials containing polarisable cations (such as Bi or Pb) and in materials close to a polar phase transition (such as $SrTiO_3$ and other perovskite structured crystals). These factors are realised in the emerging absorber SbSI which, despite its relatively wide bandgap of 1.86 eV, possesses a giant room temperature dielectric constant >10^4 (along the *c* axis) due to a ferroelectric Curie temperature around 291 K. This route has also recently been exploited in the development of ferroelectric oxide PVs, such as $KNbO_3$–$BaNi_{0.5}Nb_{0.5}O_3$ solid solutions[15]. Here, spontaneous electric polarisation promotes the separation of photoexcited carriers and enables the generation of above-bandgap photovoltages. As oxides typically possess larger bandgaps, this approach may prove especially fruitful for the identification of wide-gap defect-tolerant candidates.

Inspiration on how to achieve shallow traps in wide-gap materials can be found in bismuth oxyiodide (BiOI) and $BaZrS_3$ (E_g~1.8–1.9 eV). In BiOI, the Bi-I bonds are comparatively long (3.4 Å [Fig. 2a] vs. 3.7 Å for Pb-I in $CH_3NH_3PbI_3$)[16]. When I vacancies form, the neighbouring Bi atoms are sufficiently far apart to avoid significant orbital overlap, leading to small energy splittings in the

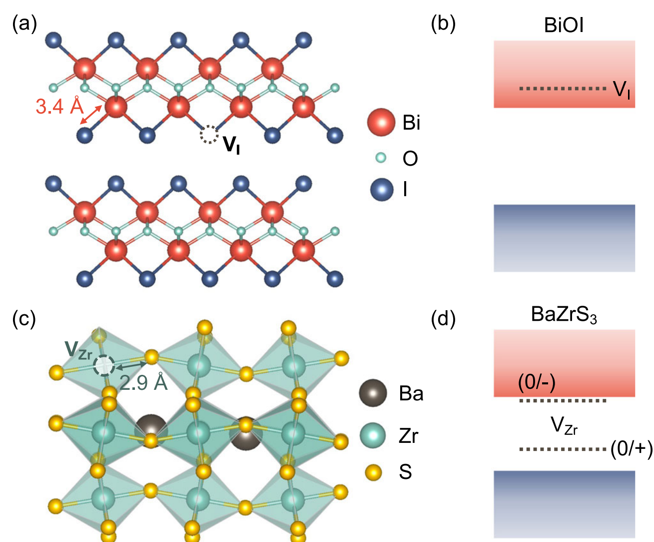

Fig. 2 | Wide-bandgap semiconductors with non-harmful traps. **a** Crystal structure and **b** band diagram of BiOI, showing the (0/+) transition level of iodide vacancies (V_I)[16]. **c** Crystal structure and **d** band diagram of $BaZrS_3$, showing the deep donor (0/+) and shallow acceptor (0/−) transition levels of zirconium vacancies (V_{Zr})[19].

bonding-antibonding combinations formed from the dangling bonds[17]. This, coupled with the moderate electron affinity of 4.1 eV, results in the V_I (0/+) donor transition level being resonant within the conduction band (Fig. 2b)[16]. The inert nature of I vacancies has been verified experimentally[18]. Preliminary defect chemistry analysis indicates that $BaZrS_3$ benefits from the flexible perovskite structure (Fig. 2c), similar to the metal halides, which 'cleans up' deep traps from the bandgap (Fig. 2d)[19]. These recent results further motivate efforts at overcoming the challenges of growing high-quality thin films of chalcogenide perovskites at low temperatures to exploit these properties in PV devices.

In conclusion, defect tolerance has allowed select low-bandgap semiconductors to achieve efficient device performance when processed by low-temperature, cost-effective methods. As a new generation of wide-bandgap semiconductors gain increasing technological significance, overcoming their unique defect challenges is of paramount importance. Promising strategies include identifying materials with high ionic dielectric constants but weak Fröhlich coupling, translating the defect chemistry of halide perovskites to alternative chalcogenide and pnictide materials, as well as using the electron affinity and ionisation potential as indicators for the dopability of the material and whether shallow traps form. These strategies, which can be used in tandem, are generalisable across all types of point defects, and not solely the vacancies discussed above as illustrative examples. Other levers for engineering defect tolerance will include built-in and applied strain and order-disorder transitions in mixed cation and mixed anion systems. Initial work will require a detailed analysis of the defects present in these materials through characterisation and calculations in order to identify parameters that are generalisable into design rules. Addressing the defect challenge for wide-gap semiconductors offers a rich opportunity to unveil new insights into chemical, structural and electronic descriptors for defect tolerance, as well as routes to push forward these materials as a cost-effective technology for energy and healthcare applications.

Alex M. Ganose[1], **David O. Scanlon**[2,3], **Aron Walsh**[1] **& Robert L. Z. Hoye**[1] ✉
[1]Department of Materials, Imperial College London, Exhibition Road, London SW7 2AZ, UK. [2]Department of Chemistry, University College London, 20 Gordon Street, London WC1H 0AJ, UK. [3]Thomas Young Centre, University College London, Gower Street, London WC1E 6BT, UK.
✉e-mail: r.hoye@imperial.ac.uk

Received: 29 March 2022; Accepted: 11 July 2022;
Published online: 11 August 2022

Data availability
No new experimental data was generated in this work.

Code availability
The data for Fig. 1c–e and Supplementary Fig. 1 were obtained from the Materials Project database[20], and the code used to extract these data and generate the plots is available from https://gist.github.com/utf/3b06d3850a6b1d643613af3bc7cb3842.

References
1. Tennyson, E. M., Doherty, T. A. S. & Stranks, S. D. Heterogeneity at multiple length scales in halide perovskite semiconductors. *Nat. Rev. Mater.* **4**, 573–587 (2019).
2. Walsh, A. & Zunger, A. Instilling defect tolerance in new compounds. *Nat. Mater.* **16**, 964–967 (2017).
3. Zunger, A., Zhang, S. B. & Wei, S.-H. Why is $CuInSe_2$ tolerant to defects and what is the origin of "Ordered Defect Structures". *AIP Conf. Proc.* **394**, 63–74 (1997).
4. Huang, Y.-T., Kavanagh, S. R., Scanlon, D. O., Walsh, A. & Hoye, R. L. Z. Perovskite-inspired materials for photovoltaics and beyond –from design to devices. *Nanotechnology* **32**, 132004 (2021).
5. Li, Z. et al. Cost analysis of perovskite tandem photovoltaics. *Joule* **2**, 1559–1572 (2018).
6. Pecunia, V., Occhipinti, L. G. & Hoye, R. L. Z. Emerging indoor photovoltaic technologies for sustainable internet of things. *Adv. Energy Mater.* **11**, 2100698 (2021).
7. Murphy, A. B. et al. Efficiency of solar water splitting using semiconductor electrodes. *Int. J. Hydrog. Energy* **31**, 1999–2017 (2006).
8. Hörantner, M. T. & Snaith, H. J. Predicting and optimising the energy yield of perovskite-on-silicon tandem solar cells under real world conditions. *Energy Environ. Sci.* **10**, 1983–1993 (2017).
9. Walukiewicz, W. Amphoteric native defects in semiconductors. *Appl. Phys. Lett.* **54**, 2094–2096 (1989).
10. Goyal, A. et al. On the dopability of semiconductors and governing material properties. *Chem. Mater.* **32**, 4467–4480 (2020).
11. Tao, S. et al. Absolute energy level positions in tin- and lead-based halide perovskites. *Nat. Commun.* **10**, 2560 (2019).
12. Kim, J., Chung, C. H. & Hong, K. H. Understanding of the formation of shallow level defects from the intrinsic defects of lead tri-halide perovskites. *Phys. Chem. Chem. Phys.* **18**, 27143–27147 (2016).
13. Persson, C., Platzer-Björkman, C., Malmström, J., Törndahl, T. & Edoff, M. Strong valence-band offset bowing of $ZnO_{1-x}S_x$ enhances p-type nitrogen doping of ZnO-like alloys. *Phys. Rev. Lett.* **97**, 146403 (2006).
14. Madelung, O. III-V Compounds. in *Semiconductors: Data Handbook* 71–172 (Springer, 2004). https://doi.org/10.1007/978-3-642-18865-7_3.
15. Grinberg, I. et al. Perovskite oxides for visible-light-absorbing ferroelectric and photovoltaic materials. *Nature* **503**, 509–512 (2013).
16. Hoye, R. L. Z. et al. Strongly enhanced photovoltaic performance and defect physics of air-stable bismuth oxyiodide (BiOI). *Adv. Mater.* **29**, 1702176 (2017).
17. Kurchin, R. C., Gorai, P., Buonassisi, T. & Stevanović, V. Structural and chemical features giving rise to defect tolerance of binary semiconductors. *Chem. Mater.* **30**, 5583–5592 (2018).
18. Huq, T. N. et al. Electronic structure and optoelectronic properties of bismuth oxyiodide robust against percent-level iodine-, oxygen-, and bismuth-related surface defects. *Adv. Funct. Mater.* **30**, 1909983 (2020).
19. Wu, X. et al. Defect tolerance in chalcogenide perovskite photovoltaic material $BaZrS_3$. *Sci. China Mater.* **64**, 2976–2986 (2021).
20. Jain, A. et al. Commentary: The materials project: a materials genome approach to accelerating materials innovation. *APL Mater.* **1**, 011002 (2013).

Acknowledgements
The authors are grateful to Chuijiang (Christina) Kong for valuable discussions, and are deeply saddened by her passing during the preparation of this comment article. A.M.G. was supported by an Engineering and Physical Sciences Research Council (EPSRC) Fellowship (No. EP/T033231/1). D.O.S acknowledges support from the European Research Council, ERC (Grant No. 758345). R.L.Z.H. would like to thank the Royal Academy of Engineering under the Research Fellowship scheme (No. RF\201718\1701) and the Engineering and Physical Sciences Research Council (EPSRC; Grant No. EP/V01498/1).

Author contributions
A.M.G., D.O.S., A.W. and R.L.Z.H. all wrote and discussed the paper together.

Competing interests
The authors declare no financial and non-financial competing interests.

Additional information
Supplementary information The online version contains supplementary material available at
https://doi.org/10.1038/s41467-022-32131-4.

Correspondence and requests for materials should be addressed to Robert L. Z. Hoye.

Peer review information *Nature Communications* thanks the anonymous reviewers for their contribution to the peer review of this work.

Reprints and permission information is available at
http://www.nature.com/reprints

Publisher's note Springer Nature remains neutral with regard to jurisdictional claims in published maps and institutional affiliations.

Open Access This article is licensed under a Creative Commons Attribution 4.0 International License, which permits use, sharing, adaptation, distribution and reproduction in any medium or format, as long as you give appropriate credit to the original author(s) and the source, provide a link to the Creative Commons license, and indicate if changes were made. The images or other third party material in this article are included in the article's Creative Commons license, unless indicated otherwise in a credit line to the material. If material is not included in the article's Creative Commons license and your intended use is not permitted by statutory regulation or exceeds the permitted use, you will need to obtain permission directly from the copyright holder. To view a copy of this license, visit http://creativecommons.org/licenses/by/4.0/.

© The Author(s) 2022